Research Article Vol. 30, No. 24 / 21 Nov 2022 / Optics Express 44085
Optics EXPRESS

Wavelength tuning of solid-state continuous-wave single frequency 1.5 μm laser by manipulating net gain spectra

ZIJIAN YAO,[1,3] YUANJI LI,[1,2,3] KUNLUN LIU,[1] JINXIA FENG,[1,2] AND KUANSHOU ZHANG[1,2,*]

[1] State Key Laboratory of Quantum Optics and Quantum Optics Devices, Institute of Opto-Electronics, Shanxi University, Taiyuan 030006, China
[2] Collaborative Innovation Center of Extreme Optics, Shanxi University, Taiyuan 030006, China
[3] Z. J. Yao and Y. J. Li contributed equally to this work.
[*] kuanshou@sxu.edu.cn

Abstract: A wavelength tuning method suitable to watt-level continuous-wave single frequency solid-state laser (CWSFL) at 1.5 μm was proposed. Based on a dual-gain-medium resonator design, the laser wavelength can be tuned by manipulating the combined net gain spectrum. Comparing with the traditional tuning method, the wavelength tuning range was eight times broader and extended to 0.438 nm, the maximum laser power was raised up to 0.64 W, which was the highest record for the 1.5 μm CWSFL to the best of our knowledge. The laser intensity noise reached the shot noise limit at the analysis frequency above 3.5 MHz. Wider wavelength tuning band of 5.58 nm can be expected when the same resonator design including two gain media with different doped concentrations was used, according to our theory.

1. Introduction

Watt-level continuous wave lasers and several hundred milliwatt (mW) continuous-wave single frequency solid-state lasers (CWSFLs) operating at 1.5 μm had been demonstrated by employing the Er^{3+} and Yb^{3+} codoped laser crystals providing higher gain and much better thermal and mechanical properties than the Er^{3+} and Yb^{3+} codoped phosphate glass [1–9]. Beyond that, the CWSFLs operating at the fiber communication spectral region also exhibited shot noise limited laser noise which was dozens dB lower than that of the fiber lasers and fiber-based master oscillator power-amplifier (MOPA) [10–12]. Consequently, this kind of laser source is a promising candidate for building large scale continuous-variable quantum communication system [13,14], demonstrating quantum information processing [15,16], and dissemination of time and frequency [17,18]. In these applications, a core requirements was the wavelength tuning capability of the laser. Specifically, the shot-noise-limited 1.5 μm carrier light sources with tunable oscillation wavelength meet the need of wavelength division multiplexing in practical quantum communication and quantum information processing, hence the costly 100 GHz-level high frequency phase modulators and the locking systems were not needed. In the field of dissemination of time and frequency, for example building optical fiber link for frequency metrology. An ultra-stable laser (USL) was always needed to provide the optical frequency standard or lock the optical frequency comb. Note that the frequency of USL had to follow the eigen-frequency of the high fineness optical cavity to get the narrowest linewidth. Consequently, the laser wavelength should be firstly tuned approaching the eigen-frequency, and then locked to it.

However, there is not yet a reliable wavelength tuning method suitable to the watt-level 1.5 μm CWSFLs suffering from the abundant and complex energy level structure of Er^{3+} ions and strong Stark effect inside the Er^{3+} doped or Er^{3+} and Yb^{3+} codoped crystalline gain media, in fact, the

#475829 https://doi.org/10.1364/OE.475829
Journal © 2022 Received 15 Sep 2022; revised 3 Nov 2022; accepted 3 Nov 2022; published 16 Nov 2022

Optics EXPRESS

emission spectra of the Er^{3+} doped or Er^{3+} and Yb^{3+} codoped laser crystals were consisted with a series of emission peaks [19], and the polarized gain spectra were also shaped as multi-peaks [2]. When the intra-cavity wavelength tuning filter, for instance etalon with low fineness, was used to tune the wavelength dependent loss of this kind of laser, e.g., tuning the spatial azimuth of etalon or birefringent filter, the additional loss was so significant that even vanishing the laser emission, and the laser wavelength was usually jumped from one peak to another before it was tuned beyond a free spectral range of the laser cavity [8,9], for example jumping from 1531 nm to 1521 nm. The methods based on high fineness filters or the combination of high fineness filter and low fineness filter locked to follow the resonator's eigen-frequency [20] were also invalid for the high insertion loss comparing with the laser gain that even vanishing the laser emission. It is worth noting that in the previous investigations, the tuning range of the 1.5 μm CWSFL based on Er^{3+} doped or Er^{3+} and Yb^{3+} codoped laser crystals had never exceeded 0.055 nm, multi-wavelength lasers or wavelength jump phenomena was more probable [1–4,21–23]. For instance, Y. J. Chen et al. demonstrated several 1.5 μm multi-mode lasers and CWSFLs with different materials including Er,Yb:YAB [2,5–8], Er,Yb:GSAO [3], Er,Yb:LPS [4], etc. The wavelengths of these lasers could jumped once the output mirror was changed with different transmission or the pump power was tuned, but neither of that can be simultaneously operated in single longitudinal mode and wavelength tuned in a broad band. Using Er^{3+} and Yb^{3+} codoped phosphate glass that offering quasi-flat emission spectra, S. Taccheo, et al. developed a 1.5 μm CWSFL allowed for single frequency operation in several tuning intervals inside the range of 1528.5-1570.2 nm by combining tunable intracavity etalon and changing the output mirror [9]. But the laser power was below 230 mW restricted by the poor thermal property of the glass, and the change of the output mirror lacks practicality. To the best of our knowledge, the continuous wavelength tuning behavior of 1.5 μm CWSFL with output power higher than 400 mW was only demonstrated by H. R. Zhu et al. with the help of a combination of two intracavity electro-optic crystals inside a twist-mode cavity, but the whole tuning range was only 0.055 nm [8].

In this paper, we propose an innovative method for wavelength tuning of the 1.5 μm CWSFL based on manipulating the net gain spectrum of a dual-gain-medium quasi-three-level laser. The wavelength tuning capability and laser power characteristics of the CWSFL were also demonstrated.

2. Mechanism of wavelength manipulation for 1.5 μm CSFL

For the 1.5-1.6 μm radiations related to the $^4I_{13/2}\rightarrow{}^4I_{15/2}$ transitions of Er^{3+} ions, the gain cross-section spectra of the gain medium can be evaluated by the equation $g(\lambda)=\beta\sigma_{em}(\lambda)-(1-\beta)\sigma_{abs}(\lambda)$ [21,24,25], where β is the inversion fraction factor, indicating the ratio of the excited Er^{3+} ions number to the total number of Er^{3+} ions. The gain cross-section spectra had been used for explicate the multi-wavelength laser operation and wavelength jumping phenomena in the quasi-three-level lasers containing one gain medium successfully [21–26].

Considering the case that there exists two gain media in one resonator, only the gain cross-section spectra is insufficient to meet the need of laser oscillating wavelength prediction. Here we introduce the net gain spectrum of the laser (G_n) with the wavelength dependent loss and the crystal parameters taken into account that can be expressed as:

$$\begin{aligned} G_n(\lambda) &= N_1 m_1 l_1[\beta_1\sigma_{em,1}(\lambda) - (1-\beta_1)\sigma_{abs,1}(\lambda)]/n_1 \\ &+N_2 m_2 l_2[\beta_2\sigma_{em,2}(\lambda) - (1-\beta_2)\sigma_{abs,2}(\lambda)]/n_2 - \delta(\lambda), \end{aligned} \tag{1}$$

where λ is the oscillating wavelength, n_i, l_i and N_i are the refractive indexes, lengths and the Er^{3+} ions number densities of the gain medium i ($i = 1,2$). $m_i = (\omega_i/\omega_0)^2$ indicate the mode evolution ratio, ω_i are the laser beam radius inside the gain medium i, ω_0 is the average laser beam radius inside the resonator. β_i, $\sigma_{abs,i}$ and $\sigma_{em,i}$ are the inversion fraction factor, stimulated absorption

Optics EXPRESS

cross-section and the stimulated emission cross-section for the gain medium i ($i = 1,2$). $\delta(\lambda)$ is the intracavity dispersive loss.

When a c-cut 1.05 mm-long Er,Yb:YAB crystal and an a-cut 1.5 mm-long Er,Yb:YAB crystal with its c-optical axis parallel to the transmission axis of the intracavity polarizer were in the resonator, and both crystals had an Er^{3+} doping concentration of 1.1% and a Yb^{3+} doping concentration of 25%, assuming that $n_1 = n_2 = 1.7508$, $\omega_1 = \omega_2 = 60$ μm, $N_1 = N_2 = 5.95 \times 10^{25}$ m^{-3}, and deriving $\delta(\lambda)$ from the dispersion characteristic of the cavity mirror coatings, the net gain spectra of the dual-gain-medium laser at different combinations of β_1 and β_2 can be simulated using Eq.(1), as well as the σ-polarized ($\sigma_{abs,1}$ and $\sigma_{em,1}$) and π-polarized spectroscopic data ($\sigma_{abs,2}$ and $\sigma_{em,2}$). Figure 1(a) gives the simulation results of the gain spectra of the dual-gain-medium laser with one inversion factor varied and the other fixed at 0.56; Fig. 1(b) gives the gain spectra of the dual-gain-medium laser with one inversion factor varied and the other fixed at 0 (the c-cut crystal not pumped); Fig. 1(c) gives the gain spectra of the combination of dual-gain-medium laser at the case that the a-cut crystal not pumped. In each figure, the gain spectra (curves) were calculated when the varied inversion factor was set as a series of number in the range from 0.2 to 0.95 with a step of 0.05. In general, only the laser at the wavelength corresponding to the peak of the net gain spectra can be oscillated via mode competition in a CWSFL. Hence the oscillating wavelengths can be predicted and was depicted as red balls in the three figures.

From Fig. 1(a), 1(b) and 1(c), one can find that there exist one or more continuous wavelength tuning band in the three cases, while the tuning band corresponding to high gain cross-section was 1529.956 nm~1530.192 nm (bandwidth: 0.236 nm) in Fig. 1(a) and located at the range of $\beta_1 = 0.55$~0.95; in Fig. 1(b), the tuning band came to be 1529.346 nm ~1529.361 nm (bandwidth: 0.02 nm) and located at the range of $\beta_2 = 0.55$~0.95; in Fig. 1(c), the tuning band came to be 1543.687 nm~1543.917 nm (bandwidth: 0.23 nm) and located at $\beta_1 = 0.8$~0.95. Obviously, in the latter two cases, wide band and high gain cross-section can not achieved simultaneously. On the contrary, the combination of dual laser crystal both being pumped solved this problem. These results can be understood via the effects of two gain media, Firstly, the gain media were amplifier for each other that raising up the ultimate output power and enhance the laser coherence. Secondly, when the dual-gain-medium scheme was used, since the two gain media had different principal axis orientation and lengths, the total gain spectra were the linear superposition of different spectra, hence can be precisely tuned by manipulating the two inversion fraction factors. More importantly, since there were more controllable variables, the tuning band for the case that using the combination of dual laser crystal can be further extended by when β_1 and β_2 were both manipulated.

The same calculations were taken repeatedly in the range that β_1 and β_2 were both varied from 0.55 to 1 with the same step size of 0.01, the oscillating laser wavelengths were then derived by finding the peaks of the net gain spectra and depicted as the contour surface shown in Fig. 2. At the top and the bottom of the contour surface, there were two continuous wavelength tuning regions, namely 1529.852 nm ~ 1530.249 nm (bandwidth: 0.397 nm) and 1529.366~1529.546 (bandwidth: 0.18 nm). Obviously, in the previous region, wider wavelength tuning span can be obtained with the same variation of β_1 or β_2. Moreover, between the two regions the oscillating wavelength experienced a steep drop, indicating a wavelength jump phenomena from 1529.852 nm to 1529.546 nm.

We also simulated the net gain spectra, as well as the predicted wavelength of the dual-gain-medium laser based on two Er,Yb:YAB crystals with different doped concentrations and lengths. One was an c-cut 1.5 mm-long Er(1.5 at. %):Yb (11 at. %):YAB crystal, and the other was a c-cut 1.05 mm-long Er(1.1 at. %):Yb(25 at. %):YAB crystal. As shown in Fig. 3, there was two continuous tuning region, one is located at the bottom that is from 1599.09 nm to 1603.37 nm, this tuning range of 4.28 nm can be achieved when β_1 is varied from 0 to 0.62 and β_2 is varied

Optics EXPRESS

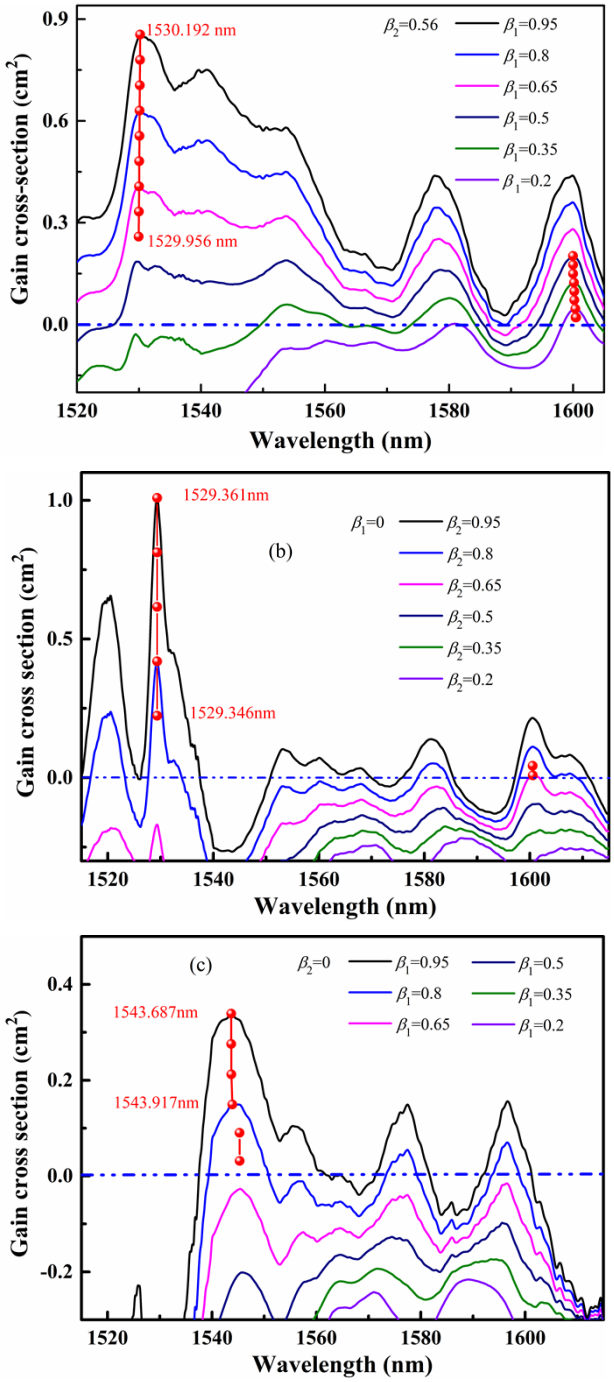

Fig. 1. Relationship between gain spectra and inversion factor for the dual-gain-medium laser with (a) one inversion factor varied and the other fixed, (b) the c-cut crystal not pumped; (c) the a-cut crystal not pumped.

Optics EXPRESS

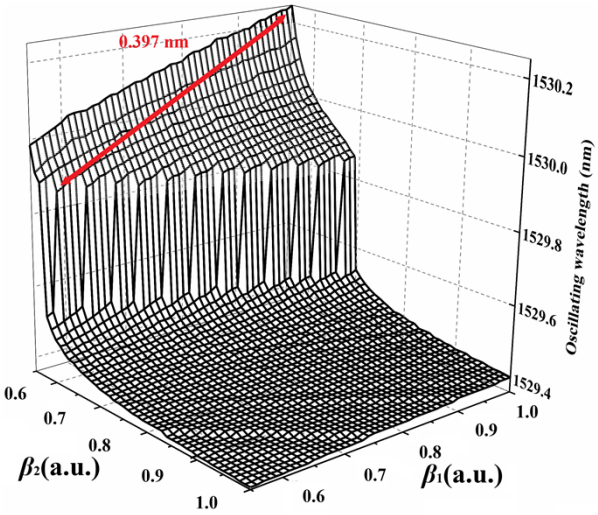

Fig. 2. Predicted oscillating wavelength of the dual-gain-medium laser based on two Er,Yb:YAB crystals with identical doped concentrations, different lengths and crystal axis orientations in the range that β_1 and β_2 were both varied from 0.55 to 1.

from 0 to 0.88; the other is located at the top (from 1607.42 nm to 1613 nm), this tuning range of 5.58 nm can be achieved when β_1 is varied from 0.18 to 0.24 and β_2 is varied from 0 to 0.24. Nevertheless, these wide tuning ranges are obtained under low power pumping, therefore the laser output should be much lower in comparison with the case shown in Fig. 2.

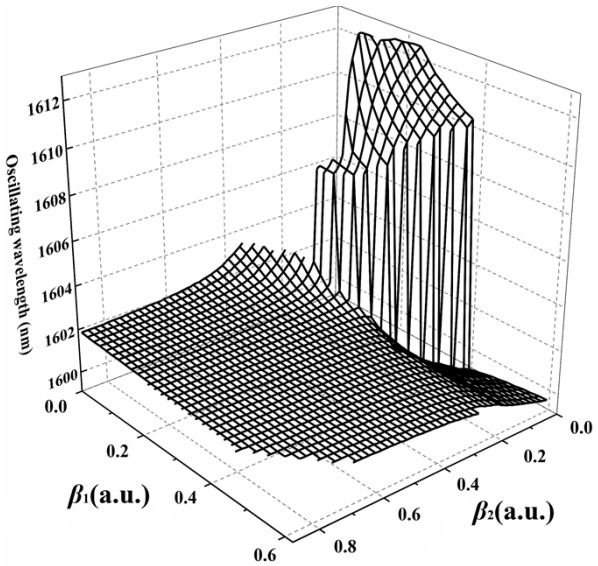

Fig. 3. Predicted oscillating wavelength of the dual-gain-medium laser based on two Er,Yb:YAB crystals with different doped concentrations and lengths in the range that β_1 and β_2 were both varied from 0 to 0.6.

Optics EXPRESS

3. Experimental setup and results

The experimental setup of the 1.5 μm tunable CWSFL was schematically shown in Fig. 4. Two pump beams with center wavelengths of 975 nm were focused onto the two composite gain media with the same waist radius of 60 μm. Both gain media were Er(1.1 at. %):Yb(25 at. %):YAB crystals that were only polished but not coated, while gain medium 1 was *c*-cut and 1.05 mm-thick, gain medium 2 was *a*-cut and 1.5 mm-thick. Four sapphire disks with one face anti-reflection (AR) coated at 1.5 μm and 976 nm were used for end cooling the gain media and reducing the Fresnel reflection loss. A 342 mm-long ring resonator consisted with four concave mirrors was designed and fabricated. M_2 and M_3 had the same radius of curvature (ROC) of 51.8 mm, M_1 and M_4 had the same ROC of 100 mm. M_1, M_2, and M_3 were high-reflection (HR) coated at 1.5 μm and high-transmission (HT) coated at 976 nm, while M_4 acting as output coupler was partial-reflection coated at 1.5 μm with a transmittance of 2%. With the insertion of a polarizer and an optical diode composed of a half-wave plate and a $Bi_3Fe_5O_{12}$ magneto-optic crystal inside the resonator, the intracavity laser was forced to propagate as a unidirectional travelling-wave, thus the continuous wave single frequency laser operation can be achieved. A home-made scanning Fabry-Perot (F-P) interferometer (cavity length: 200 mm, fineness: 260) was used to monitor the laser longitudinal mode. The power and the wavelength of the 1.5 μm CWSFL radiated from the resonator were measured using a power meter (PM) and a wavelength meter respectively. The intensity noise behavior of the 1.5 μm CWSFL was measured using a pair of self-made balanced detectors (PD_2 and PD_3) with a common mode rejection ratio of 55 dB and a spectrum analyzer.

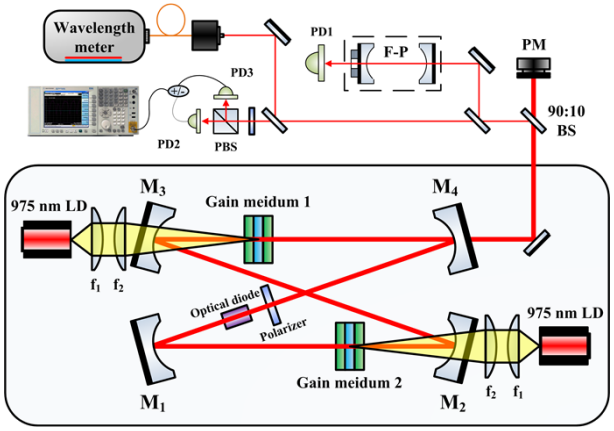

Fig. 4. Schematic of the setup of the dual-gain-medium laser.

It is well known that the inversion fraction factor β is mainly related to the pump power absorbed by the gain medium, as well as the energy transfer upconversion coefficient and excited stimulated absorption cross-section of the gain medium. Consequently, the net gain spectra of the laser can be manipulated experimentally by tuning the pump powers. Figure 5 and Fig. 6 give the measured wavelength tuning behaviors and the output property of the dual-gain-medium laser when the pump powers delivered to gain medium 1 (P_{p1}) and gain medium 2 (P_{p2}) were varied. In Fig. 5, the sphere points and the corresponding fitting curves indicate the evolution of measured oscillating wavelength data along with varying P_{p1} at the cases that P_{p2} was set as several different values in the range from 6.2 W to 7.1 W with an interval of 0.3 W. From the four sets of curves, the laser wavelength can be tuned almost linearly with varying pump powers and a whole tuning range of 1529.7524 nm~1530.1903 nm can be obtained. It should be noted that the minimum step change of the laser wavelength was 0.007 nm, which was equal to the

Optics EXPRESS

free spectral range of the resonator. From Fig. 6, it can be seen that the laser power experienced different variations during the tuning process at the cases of different P_{p2}. At $P_{p1} = 5.06$ W and $P_{p2} = 7.1$ W, the maximum power of 0.64 W, corresponding to a wavelength of 1530.0132 nm, was observed. Besides that, the laser power was always beyond 0.36 W during all the four tuning processes.

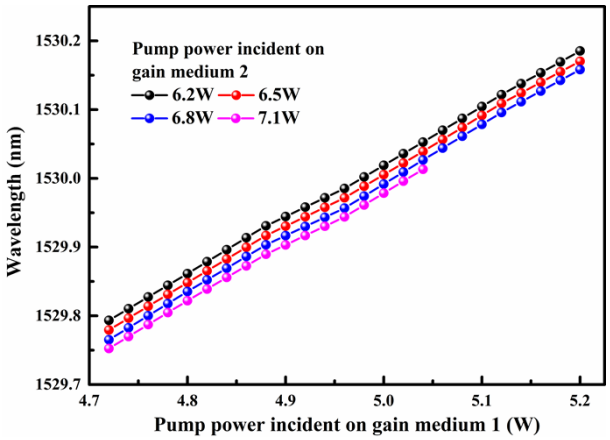

Fig. 5. Oscillating laser wavelength as functions of the pump powers incident on gain medium 1 and gain medium 2.

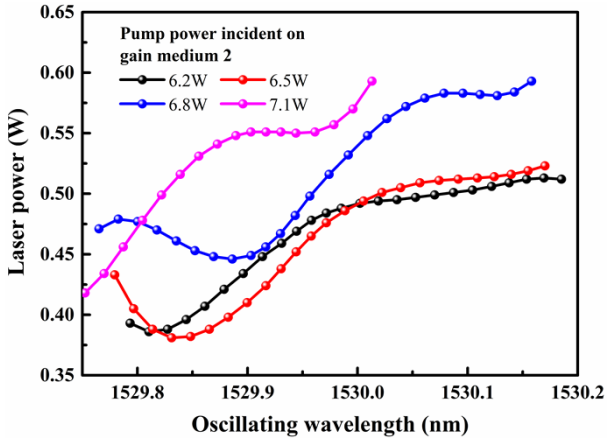

Fig. 6. Laser power as a function of the oscillating laser wavelength in different tuning processes.

Throughout the wavelength tuning, the laser longitudinal mode was monitored. Figure 7 gives the transmitted intensity of the free-running laser passing through the F-P interferometer when the laser power was 0.64 W. Note that the same transmitted intensity spectra were observed in the entire recorded pump power range shown in Fig. 5 and Fig. 6, confirming that the laser was in single frequency operation. On the contrary, mode-hop was observed outside the recorded pump power range, e.g., in the area that P_{p1} was in 5.14 W~5.23 W and P_{p2} was in 6.8 W~7.1 W, due to the severer thermal effect. Once the thermal load is reduced or the cooling scheme for the gain media is further optimized, 1.5 μm CWSFL emitting higher power can be expected according to the tendency shown in Fig. 6.

Optics EXPRESS

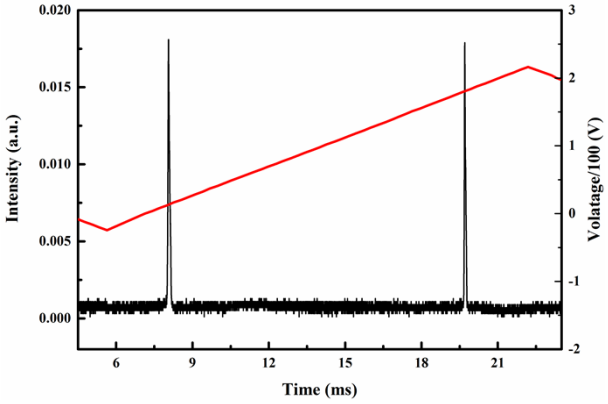

Fig. 7. Transmitted intensity of the free-running laser passing through a home-made scanning F-P interferometer.

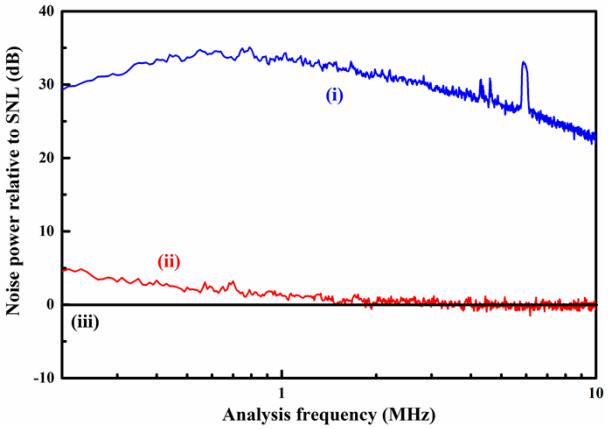

Fig. 8. Intensity noise spectra of the fiber laser (i), CWSFL (ii), and the shot noise limit (iii).

To show the advantages of the noise characteristics of the 1.5 μm tunable CWSFL, the intensity noise spectra of the free running fiber-based MOPAs (NKT Photonics, Koheras AdjustiK E15 & Koheras BoostiK sysytem E15) operating at 0.64 W output and the CWSFL operating at 1530.0132 nm were measured and depicted in Fig. 8. It can be seen that the laser intensity noise of the CWSFL reached the shot noise limit (SNL) at the analysis frequency region above 3.5 MHz. As a comparison, the intensity noises of free running fiber-based MOPAs that were usually employed in the quantum optics experiments (mainly from NKT Photonics and NP Photonics) were 20 dB or more higher than the SNL in this region when the laser was operated at a power of 0.64 W, hence additional mode cleaners was required [11,12,27–32]. Note that when the MOPA operated in the heavily saturated regime, i.e., when the seed laser intensity was much higher than the saturated intensity of the amplifier, good noise reduction can be achieved. But initial amplifiers operating in the linear and weakly saturated regime were still needed to pre-amplifying the seed power when the seed laser power was not enough high [10]. Hence low intensity noise of a MOPA was quite difficult to realize, large size and complex structure due to the implement of amplifier, mode cleaners and locking electronics were also inevitable. Note also that using self-infection technique and employing the semiconductor optical amplifier (SOA), the intensity

Optics EXPRESS

noise of the fiber laser can be suppressed and approaching the SNL, but the laser power was only 0.6~17.5 mW [33–35].

4. Conclusion

In conclusion, wavelength tuning of 1.5 μm CWSFL was demonstrated. The narrow tuning bands of the gain spectra and the frequent wavelength jump were overcome by establishing a dual-gain-medium laser cavity, and wavelength tuning was achieved by shifting the net gain spectra instead of introducing wavelength dependent loss. The wavelength tuning range was extended to 0.438 nm, which was nearly eight times broader than that of the reported 1.5 μm CWSFL using intra-cavity wavelength tuning filter. And the maximum laser power was raised up to 0.64 W, which was the highest record for the 1.5 μm CWSFL to the best of our knowledge. The laser intensity noise reached the shot noise limit at the analysis frequency above 3.5 MHz. Better wavelength tuning performance and higher laser power can be expected when the gain media combination is further optimized, for instance two or more Er,Yb:YAB crystals with different doping concentration, or the combination of two Er:GSAO crystals [3], according to our theory. Moreover, the tuning method can also be used in the 2 μm or 3 μm CWSFLs based on Ho^{3+} doped, Tm^{3+} doped, and Er^{3+} doped laser crystals.

Funding. National Natural Science Foundation of China (62175135, 61405109).

Acknowledgments. The authors gratefully acknowledge Prof. Yidong Huang and Prof. Yujin Chen for providing high quality Er,Yb:YAB crystals, essential spectroscopic data, and helpful advice.

Disclosures. The authors declare no conflicts of interest.

Data availability. Data underlying the results presented in this paper are not publicly available at this time but may be obtained from the authors upon reasonable request.

References

1. B. Denker, B. Galagan, L. Ivleval, V. Osikol, S. Sverchkov, I. voronina, J. E. Hellstrom, G. Karlsson, and F. Laurell, "Luminescent and laser properties of Yb-Er:$GdCa_4O(BO_3)_3$: a new crystal for eye-safe 1.5 μm lasers," Appl. Phys. B **79**(5), 577–581 (2004).
2. N. A. Tolstik, S. V. Kurilchik, V. E. Kisel, N. V. Kuleshov, V. V. Maltsev, O. V. Pilipenko, E. V. Koporulina, and N. I. Leonyuk, "Efficient 1 W continuous-wave diode-pumped Er,Yb:$YAl_3(BO_3)_4$ laser,," Opt. Lett. **32**(22), 3233–3235 (2007).
3. B. C. Deng, X. H. Gong, Y. J. Chen, J. H. Huang, Y. F. Lin, Z. D. Luo, and Y. D. Huang, "Polarized spectroscopic properties of disordered Er^{3+}:$Gd_2SrAl_2O_7$ crystal," Opt. Mater. Express **11**(3), 603–613 (2021).
4. J. H. Huang, Y. J. Chen, Y. F. Lin, X. H. Gong, Z. D. Luo, and Y. D. Hang, "940 mW 1564 nm multi-longitudinal-mode and 440 mW 1537 nm single-longitudinal-mode continuous-wave Er:Yb:$Lu_2Si_2O_7$ microchip lasers," Opt. Lett. **43**(8), 1643–1646 (2018).
5. Y. J. Chen, Y. F. Lin, J. H. Huang, X. H. Gong, Z. D. Luo, and Y. D. Hang, "Efficient continuous-wave and passively Q-switched pulse laser operations in a diffusion-bonded sapphire/Er:Yb:$YAl_3(BO_3)_4$/sapphire composite crystal around 1.55 μm," Opt. Express **26**(1), 419–427 (2018).
6. Y. J. Chen, Y. F. Lin, X. H. Gong, Q. G. Tan, Z. D. Luo, and Y. D. Huang, "2.0W diode-pumped Er:Yb:$YAl_3(BO_3)_4$ laser at 1.5-1.6μm," Appl. Phys. Lett. **89**(24), 241111 (2006).
7. Y. J. Li, J. X. Feng, P. Li, K. S. Zhang, Y. J. Chen, Y. F. Lin, and Y. D. Huang, "400 mW low noise continuous-wave single-frequency Er,Yb:$YAl_3(BO_3)_4$ laser at 1.55 μm," Opt. Express **21**(5), 6082–6090 (2013).
8. H. R. Zhu, L. H. Yan, Y. J. Li, and K. S. Zhang, "420 mW all solid state continouous wave single frequency tunable laser at 1542 nm," Acta Sinica Quantum Optica **25**(1), 94–99 (2019).
9. S. Taccheo, G. Sorbello, P. Laporta, G. Karlsson, and F. Laurell, "230-mW diode-pumped single-frequency Er:Yb laser at 1.5 μm," IEEE Photonics Technol. Lett. **13**(1), 19–21 (2001).
10. J. X. Feng, Y. M. Li, X. T. Tian, J. L. Liu, and K. S. Zhang, "Noise suppression, linewidth narrowing of a master oscillator power amplifier at 1.56 μm and the second harmonic generation output at 780 nm," Opt. Express **16**(16), 11871–11877 (2008).
11. Z. J. Wan, J. X. Feng, Z. N. Sun, L. T. Yao, and K. S. Zhang, "Generation of bright amplitude squeezed light at 780 nm from an extra-cavity frequency doubling," Acta Sinica Quantum Optica **20**(4), 271–274 (2014).
12. H. Zhao, J. X. Feng, J. K. Sun, Y. J. Li, and K. S. Zhang, "Real time deterministic quantum teleportation over 10 km of single optical fiber channel," Opt. Express **30**(3), 3770–3782 (2022).
13. R. Valivarthi, M. G. Puigibert, Q. Zhou, G. H. Aguilar, V. B. Verma, F. Marsili, M. D. Shaw, S. W. Nam, D. Oblak, and W. Tittel, "Quantum teleportation across a metropolitan fibre network," Nat. Photonics **10**(10), 676–680 (2016).

Optics EXPRESS

14. J. Lodewyck, M. Bloch, R. García-Patrón, S. Fossier, E. Karpov, E. Diamanti, T. Debuisschert, N. J. Cerf, R. Tualle-Brouri, S. W. McLaughlin, and P. Grangier, "Quantum key distribution over 25 km with an all-fiber continuous-variable system," Phys. Rev. A **76**(4), 042305 (2007).
15. Y. Y. Zhou, J. Yu, Z. H. Yan, X. J. Jia, J. Zhang, C. D. Xie, and K. C. Peng, "Quantum secret sharing among four players using multipartite bound entanglement of an optical field," Phys. Rev. Lett. **121**(15), 150502 (2018).
16. M. H. Wang, Y. Xiang, H. J. Kang, D. M. Han, Y. Liu, Q. Y. He, Q. H. Gong, X. L. Su, and K. C. Peng, "Deterministic distribution of multipartite entanglement and steering in a quantum network by separable states," Phys. Rev. Lett. **125**(26), 260506 (2020).
17. K. Predehl, G. Grosche, S. M. F. Raupach, S. Droste, O. Terra, J. Alnis, T. Legero, T. W. Hänsch, T. Udem, R. Holzwarth, and H. Schnatz, "A 920-Kilometer optical fiber link for frequency metrology at the 19th decimal place," Science **336**(6080), 441–444 (2012).
18. Q. Shen, J. Y. Guan, J. G. Ren, T. Zeng, L. Hou, M. Li, Y. Cao, J. J. Han, M. Z. Lian, Y. W. Chen, X. X. Peng, S. M. Wang, D. Y. Zhu, X. P. Shi, Z. G. Wang, Y. Li, W. Y. Liu, G. S. Pan, Y. Wang, Z. H. Li, J. C. Wu, Y. Y. Zhang, F. X. Chen, C. Y. Lu, S. K. Liao, J. Yin, J. J. Jia, C. Z. Peng, H. F. Jiang, Q. Zhang, and J. W. Pan, "Free-space dissemination of time and frequency with 10^{-19} instability over 113 km," Nature **610**(7933), 661–666 (2022).
19. W. X. You, Y. F. Lin, Y. J. Chen, Z. D. Luo, and Y. D. Huang, "Polarized spectroscopy of Er^{3+} ions in YAl_3 $(BO_3)_4$ crystal," Opt. Mater. **29**(5), 488–493 (2007).
20. D. Radnatarov, S. Kobtsev, S. Khripunov, and V. Lunin, "240-GHz continuously frequency-tuneable Nd:YVO_4/LBO laser with two intra-cavity locked etalons," Opt. Express **23**(21), 27322–27327 (2015).
21. Y. J. Chen, Q. Hou, Y. S. Huang, Y. F. Lin, J. H. Huang, X. H. Gong, Z. D. Luo, Z. B. Lin, and Y. D. Huang, "Efficient continuous-wave diode-pumped Er^{3+}:Yb^{3+}:$LaMgB_5O_{10}$ laser with sapphire cooling at 1.57 μm," Opt. Express **25**(16), 19320–19325 (2017).
22. K. N. Gorbachenya, V. E. Kisel, A. S. Yasukevich, V. V. Maltsev, N. I. Leonyuk, and N. V. Kuleshov, "Highly efficient continuous-wave diode-pumped Er, Yb:$GdAl_3(BO_3)_4$ laser," Opt. Lett. **38**(14), 2446–2448 (2013).
23. J. M. Serres, P. Loiko, V. Jambunatham, X. Mateos, V. Vitkin, A. Lucianetti, T. Mocek, M. Aguilo, F. Diaz, U. Griebner, and V. Petrov, "Efficient diode-pumped Er:$KLu(WO_4)_2$ laser at 1.61μm," Opt. Lett. **43**(2), 218–221 (2018).
24. L. Z. Zhang, H. F. Lin, G. Zhang, X. Mateos, J. M. Serres, M. Aguilo, F. Diaz, U. Griebner, V. Petrov, Y. C. Wang, P. Loiko, E. Vilejshikova, K. Yumashev, Z. B. Lin, and W. D. Chen, "Crystal growth, optical spectroscopy and laser action of Tm^{3+}-doped monoclinic magnesium tungstate," Opt. Express **25**(4), 3682–3693 (2017).
25. X. Mateos, S. Lamrini, K. SCholle, P. Fuhrberg, S. Vatnik, P. Loiko, I. Vedin, M. Aguiló, F. Díaz, U. Griebner, and V. Petrov, "Holmium thin-disk laser based on Ho:$KY(WO_4)_2$/$KY(WO_4)_2$ epitaxy with 60% slope efficiency and simplified pump geometry," Opt. Lett. **42**(17), 3490–3493 (2017).
26. Y. J. Chen, Y. F. Lin, J. H. Huang, X. H. Gong, Z. D. Luo, and Y. D. Hang, "Enhanced performances of diode-pumped sapphire/Er^{3+}:Yb^{3+}:$LuAl_3(BO_3)_4$/sapphire micro-laser at 1.5-1.6 μm," Opt. Express **23**(9), 12401–12406 (2015).
27. S. Steinlechner, "Squeezed light at 1550 nm," Ph.D. thesis (Gottfried Wilhelm Leibniz University, 2009).
28. M. Mehmet, T. Eberle, S. Steinlechner, H. Vahlbruch, and R. Schnabel, "Demonstration of a quantum-enhanced fiber Sagnac interferometer," Opt. Lett. **35**(10), 1665–1667 (2010).
29. J. X. Feng, Z. J. Wan, Y. J. Li, and K. S. Zhang, "Distribution of continuous variable quantum entanglement at a telecommunication wavelength over 20 km of optical fiber," Opt. Lett. **42**(17), 3399–3402 (2017).
30. Z. J. Wan, J. X. Feng, Y. J. Li, and K. S. Zhang, "Comparison of phase quadrature squeezed states generated from degenerate optical parametric amplifiers using PPKTP and PPLN," Opt. Express **26**(5), 5531–5540 (2018).
31. A. Schönbeck, F. Thies, and R. Schnabel, "13 dB squeezed vacuum states at 1550 nm from 12 mW external pump power at 775 nm," Opt. Lett. **43**(1), 110–113 (2018).
32. Y. J. Wang, W. H. Zhang, R. X. Li, L. Tian, and Y. H. Zheng, "Generation of -10.7 dB unbiased entangled states of light," Appl. Phys. Lett. **118**(13), 134001 (2021).
33. Q. L. Zhao, S. H. Xu, K. J. Zhou, C. S. Yang, C. Li, Z. M. Feng, M. Y. Peng, H. Q. Deng, and Z. M. Yang, "Broad-bandwidth near-shot-noise-limited intensity noise suppression of a single-frequency fiber laser," Opt. Lett. **41**(7), 1333–1335 (2016).
34. C. Li, S. H. Xu, X. Huang, Y. Xiao, Z. M. Feng, C. S. Yang, K. J. Zhou, W. Lei, J. L. Gan, and Z. M. Yang, "Alloptical frequency and intensity noise suppression of single-frequency fiber laser," Opt. Lett. **40**(9), 1964–1967 (2015).
35. K. J. Zhou, Q. L. Zhao, X. Huang, C. S. Yang, C. Li, E. B. Zhou, X. G. Xu, K. Y. Wong, H. H. Cheng, J. L. Gan, Z. M. Feng, M. Y. Peng, Z. M. Yang, and S. H. Xu, "kHz-order linewidth controllable 1550 nm singlefrequency fiber laser for coherent optical communication," Opt. Express **25**(17), 19752–19759 (2017).